

Dalton Transactions

Accepted Manuscript



This is an *Accepted Manuscript*, which has been through the Royal Society of Chemistry peer review process and has been accepted for publication.

Accepted Manuscripts are published online shortly after acceptance, before technical editing, formatting and proof reading. Using this free service, authors can make their results available to the community, in citable form, before we publish the edited article. We will replace this *Accepted Manuscript* with the edited and formatted *Advance Article* as soon as it is available.

You can find more information about *Accepted Manuscripts* in the [Information for Authors](#).

Please note that technical editing may introduce minor changes to the text and/or graphics, which may alter content. The journal's standard [Terms & Conditions](#) and the [Ethical guidelines](#) still apply. In no event shall the Royal Society of Chemistry be held responsible for any errors or omissions in this *Accepted Manuscript* or any consequences arising from the use of any information it contains.

Stabilization of Cu₇ Clusters in Azide networks: Syntheses, Structures and Magnetic behaviours

Subhradeep Mistry, Jean-Pascal Sutter^{2,3} and Srinivasan Natarajan¹

¹ Framework solids laboratory, Solid State and Structural Chemistry unit, Indian Institute of Science, Bangalore-560012, India.

² CNRS ; LCC (Laboratoire de Chimie de Coordination) ; 205, route de Narbonne, F-31077 Toulouse, France

³ Université de Toulouse ; UPS, INPT ; LCC ; F-31077 Toulouse, France

¹ E-mail: snatarajan@sscu.iisc.ernet.in; jean-pascal.sutter@lcc-toulouse.fr

Abstract:

Two new azide bridged copper (II) coordination polymer compounds, $[\text{Cu}_7(\text{N}_3)_{14}(\text{C}_3\text{H}_{10}\text{N}_2)(\text{C}_4\text{H}_{13}\text{N}_3)]_n$ (**I**) and $[\text{Cu}_7(\text{N}_3)_{14}(\text{C}_3\text{H}_{10}\text{N}_2)(\text{C}_5\text{H}_{15}\text{N}_3)_2]_n$ (**II**) [where $\text{C}_3\text{H}_{10}\text{N}_2$ = 1,2-diaminopropane (1,2-DAP); $\text{C}_4\text{H}_{13}\text{N}_3$ = diethylenetriamine (DETA); $\text{C}_5\text{H}_{15}\text{N}_3$ = N-2-aminoethyl-1,3-propanediamine (AEDAP)] were prepared employing a room temperature diffusion technique involving three layers. Single crystal studies reveal that both the compounds **I** and **II**, have similar connectivity forming Cu_7 clusters through end - on (EO) bonding of the azide. The Cu_7 clusters are connected through end - to - end (EE) connectivity of the azides forming three - dimensional structures. Magnetic studies confirmed the ferromagnetic interactions within the Cu_7 units and revealed the occurrence of concomitant ferro- and antiferro-magnetic interactions between these clusters. As a result **I** behaves as a weak-ferromagnet with $T_C = 10$ K.

Introduction:

The usefulness of azide $[N_3^-]$ as a bridging ligand in inorganic compounds has been well documented since a very long time.¹ There have been many azide bridged compounds, especially those of Cu(II), known in literature.² The azide bridged compounds are attractive in magnetochemistry, because (i) the azide can efficiently mediate magnetic exchanges between paramagnetic metal centers and (ii) the azide exhibits variations in the bridging modes (ESI, Scheme 1), which modulate the exchange interactions (ferro- or antiferromagnetic) between the metal ions.³

The scope of investigations involving the azide as a linker has been given a thrust by the selective use of secondary aliphatic amine molecules, which act as terminal blocking ligands.⁴ This approach provided a measure of control over the available metal coordination sites for the bridging of the azide. Recent studies involving the simultaneous use of azide along with aliphatic blocking amines gave rise to new coordination compounds of Cu(II).⁵ Many of these studies have concentrated on the use of a single blocking amine.

It occurred to us that there may be benefits in employing two different, but related, amines for the purpose of selective blocking of the coordination sites of the metal, viz., Cu(II). Our studies on the simultaneous use of 1,2 - diaminopropane (1,2-DAP) $[C_3H_{10}N_2]$ and diethylenetriamine (DETA) $[C_4H_{13}N_3]$ as well as 1,2-DAP and N-2-aminoethyl-1,3-diaminopropane (AEDAP) $[C_5H_{15}N_3]$ along with the azide gave two new copper coordination polymers, $[Cu_7(N_3)_{14}(C_3H_{10}N_2)(C_4H_{13}N_3)]_n$, **I**, and $[Cu_7(N_3)_{14}(C_3H_{10}N_2)(C_5H_{15}N_3)_2]_n$, **II**. Compounds **I** and **II**, are the first examples of copper(II) azide compounds prepared employing two different chelating amine groups with different denticity. It is important to note that both the compounds possess Cu_7 cluster units with an overall three – dimensional structure which is structurally unique among the azide bridged coordination polymers. In this manuscript, the synthesis, structure and magnetic behaviour of the compounds are presented.

Experimental section:**Caution!**

The azide and perchlorate salts are potentially explosive and adequate precautions must be taken during the handling. It is preferable to perform the experiments with small amounts of the reactants.

Synthesis:

The syntheses were carried out at room temperature employing the diffusion of chemicals involving three distinct layers. Typically, the copper perchlorate salt $\text{Cu}(\text{ClO}_4)_2 \cdot 6\text{H}_2\text{O}$ (185 mg; 0.5 mmol) with the chelating amine [0.013 ml (0.15mmol) of 1,2-DAP and 0.016 ml (0.15mmol) of DETA for compound **I**; 0.013 ml (0.15mmol) of 1,2-DAP and 0.012 ml (0.15mmol) of AEDAP for compound **II**] was taken in water (2ml), which formed the first layer (bottom of the reaction tube). A methanolic solution (2ml) of sodium azide (65mg, 1mmol) was layered on top of this mixture with a buffer layer (water + methanol, 2ml) in between (Table S1). The layers were arranged carefully to avoid any immediate mixing between the reactants. The reaction tube was kept at room temperature and the products start to form at the boundaries of the buffer layer. Good quality needle shaped dark green coloured single crystals were formed after 14 days and the products were filtered under vacuum, washed with a mixture of deionized water and methanol (1:1) and dried at ambient conditions.

Both the compounds were characterized by elemental analysis (CHN analysis), powder X-ray diffraction (PXRD) and Infra-red spectroscopy. The PXRD was recorded in the 2θ range of $5\text{--}50^\circ$ using $\text{Cu K}\alpha$ radiation (Philips X'pert). The observed PXRD patterns of the compounds **I - II** were consistent with the simulated XRD patterns generated based on the structures determined using the single crystal XRD studies (ESI, Figures S1 and S2). The

infrared (IR) spectroscopic study was carried out in the mid – IR range using KBr pellets (Perkin-Elmer, SPECTRUM 1000). The compounds **I** and **II** exhibit sharp and characteristic IR bands (ESI, Figure S3). The sharp band at $\sim 2050\text{ cm}^{-1}$ and a shoulder at $\sim 2090\text{ cm}^{-1}$ could be due to the asymmetric stretching of bridging as well as the terminal mode of the azide ligand, respectively.⁶ Medium intense peak around 1280 cm^{-1} is due to the C-N stretching mode of the aliphatic amines.

Magnetic measurements for **I** and **II** were carried out in the temperature range 2–300 K (Quantum Design MPMS 5S SQUID magnetometer). The measurements were performed on polycrystalline powders contained in gelatin capsules. The molar susceptibility (χ_M) was corrected for sample holder and for the diamagnetic contribution of all the atoms obtained from the Pascal's tables.⁷ For the field-cooled (FC), remnant (REM), and zero-field cooled (ZFC) magnetization experiments a magnetic field of 50 Oe was used. AC magnetic susceptibility studies were carried out with a AC field of 3 Oe.

Single crystal Structure determination:

The single crystal data were collected at 120(2) K on an Oxford Xcalibur (Mova) diffractometer equipped with an EOS CCD detector. The X-ray generator was operated at 50 kV and 0.8 mA using Mo K α ($\lambda = 0.71073\text{ \AA}$) radiation. The cell refinement and data reduction were accomplished using CrysAlis RED.⁸ The structure was solved by direct methods and refined using SHELX97 present in the WinGX suit of programs (version 1.63.04a).⁹ All the hydrogen positions were initially located from the difference fourier map and placed at geometrically ideal positions and refined in the riding mode. The full matrix least-squares refinement against $|F^2|$ was carried out using WinGx package of programs.¹⁰ The 1,2-DAP molecule was modelled for the disorder. The final refinements included atomic positions for all the atoms, anisotropic thermal parameters for all the non-hydrogen atoms, and isotropic thermal parameters for all the hydrogen atoms. The details of structure

determination and refinement are presented in Table 1. Important bond distances and bond angles are listed in Table S3 and S4, respectively. The CCDC numbers for the compounds are 1435115 for compound **I** and 1435116 for **II**.

Result and discussion:

Structures of $[\text{Cu}_7(\text{N}_3)_{14}(\text{C}_3\text{H}_{10}\text{N}_2)(\text{C}_4\text{H}_{13}\text{N}_3)]_n$ **I** and $[\text{Cu}_7(\text{N}_3)_{14}(\text{C}_3\text{H}_{10}\text{N}_2)(\text{C}_5\text{H}_{15}\text{N}_3)_2]_n$ **II**:

The compounds **I** and **II** have similar structures except for the presence of different blocking amines: DETA (**I**) and AEDAP (**II**). The structural description of compound **I** would be presented here as both the structures are identical.

Compound **I** has seven crystallographically independent copper atoms. Of these, two copper atoms, [Cu(1) and Cu(7)], have a distorted octahedral (O_h) geometry, four copper atoms, [Cu(2), Cu(3), Cu(4), and Cu(6)], have a distorted square pyramidal (SP) geometry, and one copper atom, [Cu(5)], has a distorted square planar geometry (ESI, Figure S4). The degree of distortion in the SP geometry in a fivefold coordination can be quantified by the distortion parameter ' τ '^[11]. A value of $\tau = 0$ generally denotes a perfect SP geometry and $0 \leq \tau \leq 0.5$ indicates a distorted SP geometry. In the present compound, values of 0.38, 0.22, 0.27 and 0.2 have been calculated for Cu(2) Cu(3), Cu(4), and Cu(6), respectively, which clearly indicates distortions to the SP geometry (Table S2). The octahedral copper centers [Cu(1) and Cu(7)] bonds with the terminal blocking amines; Cu(1) binds with 1,2-DAP and Cu(7) binds with DETA. The Cu-N bond distances exhibit two clear values with equatorial Cu-N distances in the range of 1.948(5) – 2.039(5) and apical Cu-N distances in the range 2.320(5) – 2.629(1) Å (Table S3). This suggests that the copper centers exhibit Jahn-Teller (J-T) distortions.

The copper centers are connected through the azide linkages forming a three dimensional Cu-azide polymer and both end-on (EO) and end-to-end (EE) bridges are involved. The Cu centers are all linked through the end-on (EO) azide bridges forming the

Cu₇ cluster unit. These Cu₇ clusters are connected together through both end-on (EO) and end-to-end (EE) bridging of the azide units to form the three – dimensional structure. The basic structural unit of this network consists of seven Cu centers linked by EO-azido bridges as shown in Figure 1. These Cu₇ clusters are connected together in a head-to-tail manner through EO bridges (via Cu2-N30 and Cu3-N15) in a ribbon-like arrangement Figure 2. Finally the 3-D network is realized by the interconnection of the ribbons by EE azido-bridges. The evolution of the structure from the Cu₇ cluster has been shown in Figure 1-4. There have been reports of copper compounds having Cu₇ cluster units connected through the azide ligands (Table 2), but such occurrences are rare. In both the compounds **I** and **II**, the arrangement of Cu(II) ions within the Cu₇ cluster is appears to be new. Another aspect that is noteworthy in the present structures is that the overall connectivity has a three-dimensional arrangement through the azide bonding; which is not commonly observed in copper azides.⁴

Magnetic studies:

The temperature dependence of $\chi_M T$ for **I** (χ_M stands the molar magnetic susceptibility for a Cu₇ unit) between 300 and 2 K is shown in (Figure 7). The value for $\chi_M T$ at 300 K is 3.5 cm³mol⁻¹K, which is slightly higher than the calculated value of 3.0 cm³mol⁻¹K for seven uncoupled spins with $S = \frac{1}{2}$ and $g = 2.15$, and remains unchanged down to ca 40 K. Below 25 K, the $\chi_M T$ exhibits a sharp increase to reach a value of 63.3 cm³mol⁻¹K at 9 K (14.6 cm³mol⁻¹K for $H_{DC} = 1$ kOe, ESI, Figure S9), and then decreases linearly to 17.1 cm³mol⁻¹K at 2 K. The increase of $\chi_M T$ is indicative of ferromagnetic interactions as anticipated from the structural features (vide supra). This is also supported by a Curie-Weiss analysis of the $1/\chi_M$ vs T plot between 300 and 40 K, which yielded $C = 3.33$ cm³mol⁻¹ and $\theta = 3$ K (ESI, Figure S10). However, the maximum value reached by $\chi_M T$ is much above the expected contribution for a ferromagnetic cluster of seven $S = \frac{1}{2}$ spins would reach (i.e. 7.9 cm³mol⁻¹

¹K). This, in addition to the field dependence of the maximum value for $\chi_M T$ suggested long range correlation between the Cu₇ units. Field-cooled (FC), zero-field cooled (ZFC) and remnant magnetization (REM) (Inset, Figure 7) revealed the occurrence of magnetic ordering. Based on the REM that vanishes above 10 K, the Curie temperature for **I** is $T_C = 10$ K. The temperature for the magnetic ordering was confirmed by the AC susceptibility that exhibits an out-of-phase signal below 10 K which is frequency independent (ESI, Figure S11).

The field dependence of the magnetization study indicates that **I** is not a simple ferromagnet. As can be seen in Figure 8, after the rapid increase for low fields the magnetization is small and subsequently gradually increases with the applied field. At larger fields (5 tesla) it remains much below the saturation value of *ca.* 7 μ_B expected for seven Cu(II) centers in the absence of exchange coupling. Obviously, antiferromagnetic interactions also take place within the Cu network, in agreement with the structure features. A small hysteresis loop with a coercive field of 20 Oe is observed at 2 K (Inset, Figure 8). The magnetic behaviour for compound **I** is reminiscent of a weak ferromagnet with $T_C = 10$ K, and suggests a subtle balance between ferro- and antiferromagnetic interactions leading to a small resultant ferromagnetic component.

Compound **II** does not exhibit such a transition to a weak-ferromagnet state (Figure 9). Starting from a value of 3.1 cm³mol⁻¹K for 300 K, its $\chi_M T$ versus T behaviour is characterized by a very slight increase to 3.2 cm³mol⁻¹K at 115 K followed by a gradual decrease on cooling further, reaching 1.2 cm³mol⁻¹K at 2 K, as a result of dominant antiferromagnetic interactions. However, it can be noticed that the $\chi_M T$ exhibits a small up-turn just below 10 K (Inset, ESI Figure S12), before dropping again, suggesting the concomitant growth of a ferromagnetic state much like for **I**, which however is cancelled by

anti-ferromagnetic interactions for lower T . The Curie-Weiss analysis in the temperature range 300 K to 100 K for **II** yielded $\theta = 4.3$ K and $C = 3.08 \text{ cm}^3\text{mol}^{-1}$, confirming the anticipated ferromagnetic interaction within the Cu_7 moieties (ESI, Figure S13).

The structural features of the azido coordination are known to play an essential role in the exchange interaction between two Cu centres linked by this ligand.^{3b} For instance, an EO-bridge located in equatorial position for the two Cu ions results in a much stronger exchange interaction than for the axial coordination. Moreover, ferromagnetic interactions are anticipated for Cu-N-Cu (θ) angles smaller than 105° while it becomes antiferromagnetic for larger θ . Applying these basic considerations to the Cu_7 unit suggests that ferromagnetic (F) and antiferromagnetic (AF) pathway exist between the Cu centers (Figure 5), yielding a virtual spin ground state of $S = 3/2$. The E,O-linkages present in these units within the ribbon arrangement all involve axial/equatorial coordination (Figure 2). Interestingly, among the two different E,O-linkages one exhibit large θ angles ($\text{Cu}_3\text{-N}_{15}\text{-Cu}_4^*$) with $\theta = 113.8^\circ$ in **I** and 116.6° in **II**, and the latter also have shorter apical bond lengths (Table S4-S3). The other two ($\text{Cu}_2\text{-N}_{30}\text{-Cu}_5^*$) are very close to the F/AF crossover angle with $\theta = 105.9^\circ$ in **I** and 105.1° in **II** (Figure 5 and Table S4). In both the cases weak inter- Cu_7 exchange interactions can be anticipated with the possibility of an uncertainty about the actual interaction mediated by the N_{30} -bridges.

Though the overall behaviours in **I** and **II** appear to be similar, resulting from long range correlations, the distinct behaviour for the two compounds suggests a subtle influence of the structural arrangement towards the magnetic interactions between the Cu(II) centers, with azido bridges involved in the interconnection between the Cu_7 units. Based on the structural features discussed above, a likely origin might be the linkages between Cu_3 and Cu_4 by N_{15} . For **II**, the angle is more open and hence should favour a slightly larger AF

interaction between the Cu_7 than for **I** (Figure 5 and Table S4). A second possibility is the inter-ribbon connectivity through the octahedral copper atoms $\text{Cu}(1)$ and $\text{Cu}(7)$, via end to end (EE) type bonding of the azide. Thus, the azide molecule ($\text{N}_{42}\text{-N}_{43}\text{-N}_{44}$) [Figure 6 and ESI, Figure S8] has the EE connectivity involving three copper centers, viz, $\text{Cu}(7)$, $\text{Cu}(1)$, and $\text{Cu}(6)$, and the azide ($\text{N}_{12}\text{-N}_{13}\text{-N}_{14}$) [Figure 6 and ESI, Figure S8] links to four different copper centers, viz, $\text{Cu}(1)$, $\text{Cu}(2)$, $\text{Cu}(3)$ and $\text{Cu}(7)$. A noticeable difference between **I** and **II** is found by careful examination of the torsional angles of these two azides (Table 3). The azide ($\text{N}_{42}\text{-N}_{43}\text{-N}_{44}$) exhibits torsional angle variation in the range of -40.7° to -168.2° in compound **I**, whereas the observed torsional angle for the same azide in **II** is in the range of -24.9° to -157.9° . As can be seen, there is a considerable variation in the torsional angle involving the EE azide molecules, which are primarily responsible for the inter-cluster exchanges.¹² A similar situation is also noted in the other end of the cluster connection. Here, the azide ($\text{N}_{12}\text{-N}_{13}\text{-N}_{14}$), exhibit a torsional angle variation in the range of -38.8° to 168.8° for **I** and -26.8° to 177.5° for **II** (Table 3). The EE-azido-bridges are known to favour antiferromagnetic interactions but a modulation of this exchange by the torsional angle of its coordination to Cu centers is very likely.¹²

A single ferro - or anti-ferromagnetic interaction cannot account for the low temperature behaviours. The inter-cluster interactions clearly result from a concomitant contribution of the two types of interaction which are differently balanced for the two compounds. This suggests that the E,E and the EO-azido ligands bridging the Cu_7 units may mediate either through ferro - or anti-ferromagnetic interactions depending on subtle variations of their geometrical parameters. As seen above, two possibilities can be identified. However, these systems are too complex to allow any magneto-structural correlation.

Conclusion:

The syntheses and structures of two new azide coordination polymers, $[\text{Cu}_7(\text{N}_3)_{14}(\text{C}_3\text{H}_{10}\text{N}_2)(\text{C}_4\text{H}_{13}\text{N}_3)]_n$ (**I**) and $[\text{Cu}_7(\text{N}_3)_{14}(\text{C}_3\text{H}_{10}\text{N}_2)(\text{C}_5\text{H}_{15}\text{N}_3)_2]_n$ (**II**) containing Cu^{II}_7 metal cluster with two different, but related, aliphatic amines have been accomplished. The overall three – dimensional structures, comprising of Cu_7 cluster units, is unique. One of the observations of the present study is that the compounds **I** and **II**, are the first examples of copper(II) azide compounds prepared employing two different chelating amine groups with different denticity. The amines only act as the coordinating ligands for the copper centers and are terminal. It is likely that the use of two different amines having different lengths could have played a part in the stabilization of Cu_7 clusters. The number of examples on the use of different amine for the stabilization of copper-azide compounds is not many and our continuing investigations indicates many related copper azide compounds can be prepared by this approach. We are still evaluating the different roles of the amine molecules. Magnetic studies and structural features indicate a quite intricate exchange coupled system with azido EO- and EE-bondings involved as both ferro - and anti-ferromagnetic exchange pathways. For EE-bridges exchange interaction is possibly modulated by the Cu-N_3 torsional angles. As an interesting consequence of such competitive interactions, compound **I** behaves as a weak ferromagnet with $T_C = 10$ K. It is likely that newer copper clusters and assemblies can be formed by the strategy of the use of two or more blocking amines.

Acknowledgement:

SN thanks Department of Science and Technology (DST), and Council of Scientific and Industrial Research (CSIR), Government of India, for the award of a research grants. DST is also thanked for the award of J C Bose National fellowship. JPS acknowledges CEFIPRA/IFCPAR (Indo-French Center for the Promotion of Advanced Research) for support.

Supporting Information Available:

Various mode of azide bridging (Scheme 1); Synthesis composition employed for the preparation of compounds **I- II** (Table S1); calculated ' τ ' and other parameters for compound **I-II** (Table S2); Selected observed bond distances in the compounds **I – II** (Table S3); Cu(II)-N_{EO(1,1)}-Cu(II) bond angle table for compound **I –II** (Table S4); Powder XRD patterns of the compound **I** (Fig. S1); Powder XRD patterns of the compound **II** (Fig. S2); IR spectra for the compounds **I-II** (Fig. S3); Asymmetric unit in compound **I** (Fig. S4); Asymmetric unit in compound **II** (Fig. S5); 3D view of compound **I** from crystallographic axis *a* (Fig. S6); 3D view of compound **II** from crystallographic axis *a* (Fig. S7); View of various azide connectivity present in compound **I**. (Fig. S8); Compound **I**: $\chi_M T = f(T)$ for $H_{DC} = 1$ kOe (in black) and 50 Oe (in red). (Fig. S9); $1/\chi_M = f(T)$ and Curie-Weiss best fit (considered *T* range, 300 – 40 K) (Fig. S10); The thermal variation of the in- (χ_M') and out-of-phase (χ_M'') magnetic susceptibility for **I** obtained for $H_{AC} = 3$ Oe and frequency of 100 Hz, 499 Hz, and 997 Hz (Fig. S11); The thermal variation of the magnetic susceptibility (χ_M) for compound **II**, (Inset) Variation of $\chi_M T$ as function of temperature (50 – 2 K) (Fig. S12); $1/\chi_M = f(T)$ and Curie-Weiss best fit (considered *T* range, 300 – 100 K) (Fig. S13).

References:

- (a) L. O. Brockway, L. Pauling, *Proc. Natl. Acad. Sci., U.S.A.*, 1933, **19**, 860. (b) R. Huisgen, *Angew. Chem., Int. Ed.*, 1963, **2**, 633.
- (a) S. Mukherjee, B. Gole, R. Chakrabarty, P. S. Mukherjee, *Inorg. Chem.*, 2009, **48**, 11325. (b) Z-G. Gu, Y-F. Xu, X-J. Yin, X-H. Zhou, J-L. Zuo, X-Z. You, *Dalton Trans.*, 2008, 5593. (c) Z-G. Gu, J-L. Zuo, X-Z. You, *Dalton Trans.*, 2007, 4067. (d) X-M. Zhang, Y-Q. Wang, Y. Song, E-Q. Gao, *Inorg. Chem.*, 2011, **50**, 7284. (e) A. M. Morsy, A. Youssef, A. Escuer, F. A. Mautner, L. Öhrström, *Dalton Trans.* 2008, 3553. (f) Z-G. Gu, J-J. Na, B-X. Wang, H-P. Xiao, Z. Li, *Cryst.Eng.Comm.*, 2011, **13**, 6415. (g) S. Mukherjee, P. S. Mukherjee, *Cryst. Growth Des.*, 2014, **14**, 4177. (h) X. Liu, P. Cen, H. Li, H. Ke, S. Zhang, Q. Wei, G. Xie, S. Gao, *Inorg. Chem.*, 2014, **53**, 8088. (i) A. Chakraborty, L.S. Rao, A. K. Manna, S. K. Pati, J. Ribas, T. K. Maji, *Dalton Trans.* 2013, **42**, 10707.
- (a) O. Kahn, *Inorganica Chimica Acta.*, 1982, **62**, 3. (b) E. Ruiz, J. Cano, S. Alvarez, P. Alemany, *J. Am. Chem. Soc.*, 1998, **120**, 11122. (c) Q-X. Jia, M-L. Bonnet, E-Q. Gao, V. Robert, *Eur. J. Inorg. Chem.*, 2009, 3008. (d) A. Chakraborty, L.S. Rao, A. K. Manna, S. K. Pati, J. Ribas, T. K. Maji, *Dalton Trans.* 2013, **42**, 10707. (e) S. Triki, C. J. Gómez-García, E. Ruiz, J. Sala-Pala, *Inorg. Chem.*, 2005, **44**, 5501.
- S. Mukherjee, P. S. Mukherjee, *Acc. Chem. Res.*, 2013, **46** (11), 2556.
- (a) K. C. Mondal, P. S. Mukherjee, *Inorg. Chem.* 2008, **47**, 4215. (b) S. Mukherjee, B. Gole, Y. Song, P. S. Mukherjee, *Inorg. Chem.*, 2011, **50**, 3621. (c) S. Mukherjee, P. S. Mukherjee, *Inorg. Chem.*, 2010, **49**, 10658. (d) S. Mukherjee, P. S. Mukherjee, *Dalton Trans.*, 2013, **42**, 4019.

6. (a) T. C. Stamatatos, G. S. Papaefstathiou, L. R. MacGillivray, A. Escuer, V. Ramon, E. Ruiz, S. P. Perlepes, *Inorg Chem.*, 2007, **46**, 8843. (b) P. S. Mukherjee, S. Dalai, G. Mostafa, T-H. Lu, E. Rentschler, N. R. Chaudhuri, *New J. Chem.*, 2001, **25**, 1203.
7. O. Kahn, *Molecular Magnetism*. VCH: Weinheim, 1993.
8. Oxford Diffraction (2009). CrysAlis Pro Red, version 1.171.33.34d; Oxford Diffraction Ltd.: Abingdon, Oxfordshire, England.
9. G. M. Sheldrick, SHELXS-97, Program for crystal structure solution and refinement; University of Göttingen: Göttingen, Germany, 1997.
10. L. J. J. Farrugia, *Appl. Crystallogr.*, 1999, **32**, 837.
11. (a) A.W. Addison, T.N. Rao, *J. Chem. Soc., Dalton Trans.* 1984, 1349. (b) S. Bhattacharya, U. Sanyal, S. Natarajan, *Cryst. Growth Des.* 2011, **11**, 735.
12. (a) J. Ribas, A. Escuer, M. Monfort, R. Vicente, R. Cortés, L. Lezama, T. Rojo, *Coord. Chem. Rev.*, 1999, **193-195**, 1027. (b) P. S. Mukherjee, T. K. Maji, G. Mostafa, T. Mallah, N. R. Chaudhuri, *Inorg. Chem.* 2000, **39**, 5147.
13. (a) X. Liu, J. A. McAllister, M. P. De Miranda, B. J. Whitaker, C. A. Kilner, M. Thornton-Pett, M. A. Halcrow, *Angew. Chem. Int. Ed.*, 2002, **41**, 756. (b) J. A. Real, G. De Munno, R. Chiappetta, M. Julve, F. Lloret, Y. Journaux, J.-C. Colin, G. Blondin, *Angew. Chem. Int. Ed.*, 1994, **33**, 1184. (c) X. Liu, J. A. McAllister, M. P. de Miranda, E. J. L. McInnes, C. A. Kilner, M. A. Halcrow, *Chem. Eur. J.* 2004, **10**, 1827. (d) S. Triki, F. Thétiot, J.S. Pala, S. Golhen, J.M. Clemente-Juan, C. J. Gómez-García, E. Coronado, *Chem. Commun.*, 2001, 2172. (e) A. Igashira-Kamiyama, J. Fujioka, S. Mitsunaga, M. Nakano, T. Kawamoto, T. Konno, *Chem. Eur. J.*, 2008, **14**, 9512. (f) M. Gottschaldt, R. Wegner, H. Görls, E-G. Jäger, D. Klemm, *Eur. J. Inorg. Chem.*, 2007, 3633. (g) Y. Xu, P. Xia, X. Wang, W. Wei, F. Zhanga, C. Hu, *Cryst. Eng. Comm.*, 2011, **13**, 2820. (h) H. Arora, J. Cano, F. Lloret, R. Mukherjee, *Dalton Trans.*,

2011, **40**, 10055. (i) Z-Y Liu, H-Y Zhang, E-C Yang, Z-Y Liua, X-J Zhao, *Dalton Trans.*, 2015, **44**, 5280. (j) S. S. Tandon, S. D. Bunge, L. K. Thompson, *Chem. Commun.*, 2007, 798. (k) J-P Tong, X-J Sun, J. Tao, R-B Huang, L-S Zheng, *Inorg. Chem.*, 2010, **49**, 1289. (l) J. J. Henkelis, L. F. Jones, M. P. de Miranda, C. A. Kilner, M. A. Halcrow, *Inorg. Chem.*, 2010, **49**, 11127. (m) E-C Yang, Y-Y Zhang, Z-Y Liu, X-J Zhao, *Inorg. Chem.*, 2014, **53**, 327. (n) C-D Zhang, S-X Liu, C-Y Sun, F-J Ma, Z-M Su, *Cryst. Growth Des.* 2009, **9**, 3655. (o) J. A. Przyojski, N. N. Myers, H. D. Arman, A. Prosvirin . K. R. Dunbar, M. Natarajan, M. Krishnan, S. Mohan, J. A. Walmsley, *Journal of Inorganic Biochemistry*, 2013, **127**, 175. (p) H-X Li, Z-G Ren, D. Liu, Y.Chen, J-P Lang, Z-P Cheng, X-L Zhu, B. F. Abrahams, *Chem. Commun.*, 2010, **46**, 8430. (q) D-Y Wu, W. Huang, L. Liu, Y-X Han, G-H Wu, *Inorg. Chem. Comm.*, 2011, **14**, 667. (r) Y. Ma, A-L Cheng, B. Tanga, E-Q Gao, *Dalton Trans.*, 2014, **43**, 13957.

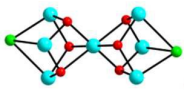
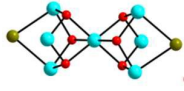
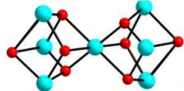
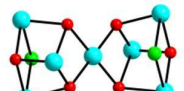
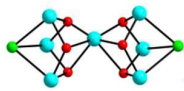
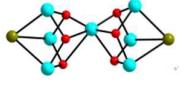
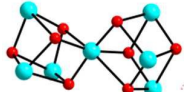
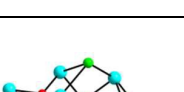
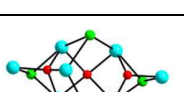
Table 1: Crystal data and structure refinement parameters for the compounds **I** and **II**.

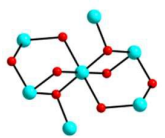
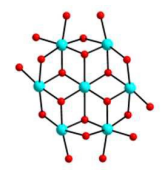
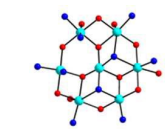

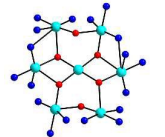
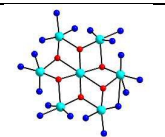
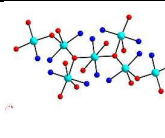
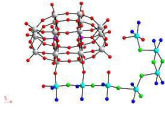
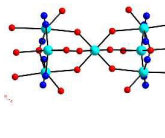
Structural parameter	I	II
Empirical formula	C ₇ H ₂₂ N ₄₇ Cu ₇	C ₈ H ₂₄ N ₄₇ Cu ₇
Crystal system	monoclinic	monoclinic
Space group	<i>P2₁/n</i> (no.11)	<i>P2₁/n</i> (no.11)
<i>a</i> (Å)	12.2870(3)	12.333(2)
<i>b</i> (Å)	13.4591(3)	13.499(3)
<i>c</i> (Å)	23.1223(5)	23.155(4)
<i>α</i> (°)	90.00	90.00
<i>β</i> (°)	92.809(2)	93.365(9)
<i>γ</i> (°)	90.00	90.00
<i>V</i> (Å ³)	3819.19(15)	3848.3(12)
<i>Z</i>	4	4
T/K	120(2)	120(2)
<i>ρ</i> (calc/gcm ⁻³)	2.103	2.112
<i>μ</i> (mm ⁻¹)	3.904	3.876
<i>λ</i> (Mo K α /Å)	0.71073	0.71073
θ range (°)	2.44 to 26.00	1.75 to 26.00
Rint	0.0464	0.0609
R indexes [<i>I</i> > 2 σ (<i>I</i>)]	R ₁ = 0.0560; wR ₂ = 0.1290	R ₁ = 0.0634; wR ₂ = 0.1398
R indexes (all data)	R ₁ = 0.0649; wR ₂ = 0.1343	R ₁ = 0.0718; wR ₂ = 0.1432

$$R_1 = \frac{\sum |F_o| - |F_c|}{\sum |F_o|}; \quad wR_2 = \left\{ \frac{\sum [w(F_o^2 - F_c^2)]}{\sum [w(F_o^2)^2]} \right\}^{1/2}. \quad w = 1/[\rho^2(F_o)^2 + (aP)^2 + bP].$$

$$P = [\max(F_o, 0) + 2(F_c)^2]/3 \text{ where } a = 0.0486 \text{ and } b = 34.2762 \text{ for I, } a = 0.0315 \text{ and } b = 59.7497 \text{ for II.}$$

Table 2: Reported Cu^{II}₇ reported in literature and its magnetic property:

S. No.	Compound	Blocking agent used	Lattice parameter		Magnetic behaviour	Figure (Cu ^{II} ₇)	Ref
			a(Å)	b(Å)			
1.	[Cu ₃ (Hpz ^{tBu}) ₆ (μ ₃ -Cl)(μ ₃ -OH) ₃] ₂ CuCl ₆	Hpz ^{tBu} = 5-tert-Butylpyrazole	a(Å)	12.3485(1)	Antiferromagnetic		13a
			b(Å)	15.8875(1)			
			c(Å)	17.6179(2)			
			α(°)	116.6860(4)			
			β(°)	103.7656(4)			
			γ(°)	91.3234(7)			
2.	[Cu ₇ (bipym)(OH) ₈ (H ₂ O) ₂](NO ₃) ₈ · H ₂ O	2,2'-bipyridin	a(Å)	11.553(7)	Ferromagnetic	-	13b
			b(Å)	13.164(7)			
			c(Å)	13.419(8)			
			α(°)	70.66(4)			
			β(°)	82.21(5)			
			γ(°)	64.14(4)			
3.	[Cu ₃ (Hpz ^{tBu}) ₆ (μ ₃ -Br)(μ ₃ -OH) ₃] ₂ CuBr ₆	3{5}-tert-butylpyrazole	a(Å)	12.3229(1)	Antiferromagnetic		13c
			b(Å)	15.9091(2)			
			c(Å)	32.0710(4)			
			α(°)	90			
			β(°)	97.4540(5)			
			γ(°)	90			
4.	[Cu ₃ (Hpz ^{tBu}) ₆ (κ ¹ , μ ₃ -NO ₃)(μ ₃ -OH) ₃] ₂ Cu[NO ₃] ₆	3{5}-tert-butylpyrazole	a(Å)	14.2664(2)	Antiferromagnetic		13c
			b(Å)	16.5432(2)			
			c(Å)	16.5838(2)			
			α(°)	119.4961(6)			
			β(°)	97.7594(6)			
			γ(°)	95.8939(5)			
5.	[Cu ₇ (OH) ₆ Cl ₂ (pn) ₆ (H ₂ O) ₂](C(CN) ₃) ₄ Cl ₂	1,3-diaminopropane	a(Å)	24.8994(3)	Antiferromagnetic		13d
			b(Å)	11.9801(2)			
			c(Å)	21.4298(3)			
			α(°)	90			
			β(°)	112.14(6)			
			γ(°)	90			
6.	[Cu ₇ (μ ₃ -OH) ₆ (μ ₃ -Cl) ₂ (1-pends) ₃]	d-penicillamine	a(Å)	15.0898(9)	Antiferromagnetic		13e
			b(Å)	15.0898(9)			
			c(Å)	27.315(2)			
			α(°)	90			
			β(°)	90			
			γ(°)	120			
7.	[Cu ₇ (μ ₃ -OH) ₆ (μ ₃ -Br) ₂ (d-pends) ₃]	d-penicillamine	a(Å)	15.1101(8)	Antiferromagnetic		13e
			b(Å)	15.1101(8)			
			c(Å)	27.6093(19)			
			α(°)	90			
			β(°)	90			
			γ(°)	120			
8.	[Cu ₇ (η ⁴ -3a) ₃ (η ⁴ -H3a)(η ³ -H3a)(acac)]	6-(β-keto-enamino)-6-deoxy-1,2- <i>o</i> -isopropylidene-α-D-glucofuranoses	a(Å)	19.1223(10)	-		13f
			b(Å)	23.912(2)			
			c(Å)	28.021(2)			
			α(°)	90			
			β(°)	90			
			γ(°)	90			
9.	[Cu ₇ O(OH) ₂ Cl ₄ (bdpz) ₆ (H ₂ O)(DMF) ₃].5DMF	4-bromo-3,5-dimethylpyrazolate	a(Å)	24.3342(13)	Antiferromagnetic		13g
			b(Å)	22.3283(12)			
			c(Å)	14.4168(8)			
			α(°)	90			
			β(°)	90			
			γ(°)	90			
10.	[Cu ₇ O(OH) ₂ Cl ₄ (bdpz) ₆ (H ₂ O)(DMAC) ₃].	4-bromo-3,5-dimethylpyr	a(Å)	23.261(4)	-		13g
			b(Å)	13.8565(19)			
			c(Å)	24.237(4)			
			α(°)	90			

	2DMAC DMAC = dimethylacetamid e	azolate	$\beta(^{\circ})$ $\gamma(^{\circ})$	106.222(2) 90			
11.	$[\text{Cu}^{\text{II}}_7(\text{L})_4(\mu_3\text{-OH})_2(\text{H}_2\text{O})_2\text{-}(\text{DMF})_2][\text{ClO}_4]_4 \cdot 4\text{H}_2\text{O}$	[N-(2-pyridylethyl)-iminodipropionate(2-)]	a(Å) b(Å) c(Å) $\alpha(^{\circ})$ $\beta(^{\circ})$ $\gamma(^{\circ})$	13.7503(9) 21.2623(13) 15.0633(9) 90 114.992(10) 90	Antiferromagnetic		13h
12.	$\{[\text{Cu}_7(\text{H}_2\text{O})_4(\mu_3\text{-OH})_6(\text{ade})_2\text{-}(\text{sip})_2] \cdot 2.5\text{H}_2\text{O}\}_n$	ade = adeninate and sip = 5-sulfoisophth alate	a(Å) b(Å) c(Å) $\alpha(^{\circ})$ $\beta(^{\circ})$ $\gamma(^{\circ})$	7.7233(11) 12.3827(17) 12.4646(17) 68.448(2) 78.217(3) 81.382(3)	Antiferromagnetic + Ferromagnetic		13i
13.	$[(\text{L}3\text{-}6\text{H})\text{Cu}_7(\mu_3\text{OCH}_3)(\mu_3\text{-OH})_2(\text{CH}_3\text{OH})_2(\text{NO}_3)(\text{H}_2\text{O})(\text{N}_3)_2]_2(\text{NO}_3)_4 \cdot 9\text{H}_2\text{O}$		a(Å) b(Å) c(Å) $\alpha(^{\circ})$ $\beta(^{\circ})$ $\gamma(^{\circ})$	14.0485(12) 15.7647(14) 15.772(2) 116.174(2) 108.739(2) 98.205(2)	Antiferromagnetic		13j
14.	$[\text{Cu}_7(\text{H}_2\text{L}')(\text{HL}')_2(\text{Meppz})(\text{H}_2\text{O})\text{Cl}_4]$	3-(2-hydroxy-5methylphenyl)pyrazole (H_2Meppz)	a(Å) b(Å) c(Å) $\alpha(^{\circ})$ $\beta(^{\circ})$ $\gamma(^{\circ})$	22.666(1) 20.678(1) 32.502(1) 90 90 90	Antiferromagnetic		13k
15.	$[\text{Cu}_7(\mu_3\text{-OH})_4(\mu\text{-OCH}_2\text{CF}_3)_2(\mu\text{-L})_6][\text{BF}_4]_2$	3-pyridyl-5-tert-butylpyrazole	a(Å) b(Å) c(Å) $\alpha(^{\circ})$ $\beta(^{\circ})$ $\gamma(^{\circ})$	11.1372(8) 15.6751(11) 16.6996(12) 116.003(3) 100.297(4) 92.519(4)	Antiferromagnetic		13l
16.	$[\text{Cu}_7(\mu_3\text{-OH})_4(\mu\text{-OMe})_2(\mu\text{-L})_6]\text{Cl}_2 \cdot x\text{CH}_2\text{Cl}_2$	3-pyridyl-5-tert-butylpyrazole	a(Å) b(Å) c(Å) $\alpha(^{\circ})$ $\beta(^{\circ})$ $\gamma(^{\circ})$	30.7871(3) 30.7871(3) 27.0562(4) 90 90 120	Antiferromagnetic		13l
17.	$\{[\text{Cu}_7(\text{H}_2\text{O})_2(\mu\text{-OH})_2(\mu_3\text{-OH})_2(\text{ta})_4(\text{sip})_2] \cdot 7\text{H}_2\text{O}\}_n$	1,2,3-triazolate and 5-sulfoisophth alate	a(Å) b(Å) c(Å) $\alpha(^{\circ})$ $\beta(^{\circ})$ $\gamma(^{\circ})$	7.4565(8) 17.0215(17) 17.1578(17) 90 97.280(2) 90	Antiferromagnetic		13m
18.	$[\text{Cu}_7(\text{Phen})_7(\text{H}_2\text{O})_4\text{Cl}_8][\text{P}_2\text{W}_{18}\text{O}_{62}] \cdot 6\text{H}_2\text{O}$	1,10-phenanthroline	a(Å) b(Å) c(Å) $\alpha(^{\circ})$ $\beta(^{\circ})$ $\gamma(^{\circ})$	14.1255(9) 17.2468(11) 28.2613(18) 101.025(10) 99.0110(10) 92.7320(10)	Ferromagnetic		13n
19.	$[\text{Cu}_7(\text{C}_7\text{H}_5\text{N}_2)_6(\mu_3\text{-OH})_6(\mu_2\text{-H}_2\text{O})_2(\mu_2\text{-CH}_3\text{OH})_4](\text{CH}_3\text{COO})_2 \cdot 2\text{C}_7\text{H}_8 \cdot 6\text{CH}$	7-azaindole	a(Å) b(Å) c(Å) $\alpha(^{\circ})$ $\beta(^{\circ})$	13.475 (4) 12.945 (4) 23.392 (7) 90 91.232 (6)	Antiferromagnetic		13o

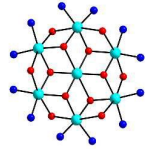
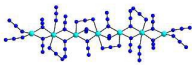
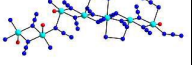
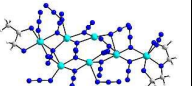
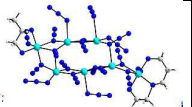
	$_3\text{OH}$		$\gamma(^{\circ})$	90			
20.	$[\text{Cu}_7(\text{OH})_2(\text{OAc})_6(\text{dmpz})_6(\text{EtOH})_6]$	3,5-dimethyl-4-nitro-1H-pyrazole)	a(Å)	13.475(4)	-		13p
			b(Å)	12.945(4)			
			c(Å)	23.392(7)			
			$\alpha(^{\circ})$	90			
			$\beta(^{\circ})$	91.232(6)			
			$\gamma(^{\circ})$	90			
21.	$(\text{L}')_2[\text{Cu}_7(\text{N}_3)_{16}]$	2-[(pyridin-2-ylmethylene)-amino] ethanol	a(Å)	7.5032(15)	Ferromagnetic		13q
			b(Å)	13.897(3)			
			c(Å)	14.899(3)			
			$\alpha(^{\circ})$	106.96(3)			
			$\beta(^{\circ})$	101.06(3)			
			$\gamma(^{\circ})$	105.29(3)			
22.	$[\text{Cu}_7(\text{L}_2)_2(\text{N}_3)_{14}]_n$	1-carboxylatome thyl-4,4'-dimethylenedi pyridinium	a(Å)	10.677(2)	Ferromagnetic		13r
			b(Å)	11.349(2)			
			c(Å)	13.181(3)			
			$\alpha(^{\circ})$	115.25(3)			
			$\beta(^{\circ})$	96.79(3)			
			$\gamma(^{\circ})$	106.40(3)			
15.	$[\text{Cu}_7(\text{N}_3)_{14}(\text{C}_3\text{H}_{10}\text{N}_2)(\text{C}_4\text{H}_{13}\text{N}_3)]_n$	1,2-diaminopropane + Diethylenetriamine	a(Å)	12.2870(3)	Ferromagnetic		This work
			b(Å)	13.4591(3)			
			c(Å)	23.1223(5)			
			$\alpha(^{\circ})$	90.00			
			$\beta(^{\circ})$	92.809(2)			
			$\gamma(^{\circ})$	90.00			
16.	$[\text{Cu}_7(\text{N}_3)_{14}(\text{C}_3\text{H}_{10}\text{N}_2)(\text{C}_5\text{H}_{15}\text{N}_3)_2]_n$	1,2-diaminopropane + N-2-Aminoethyl-1,3-propanediamine	a(Å)	12.333(2)	Ferromagnetic		This work
			b(Å)	13.499(3)			
			c(Å)	23.155(4)			
			$\alpha(^{\circ})$	90.00			
			$\beta(^{\circ})$	93.365(9)			
			$\gamma(^{\circ})$	90.00			

Table 3: Important torsional angles involving azide N₄₂-N₄₃-N₄₄ and N₁₂-N₁₃-N₁₄, in compound **I** and **II**.

Moiety	angle	Moiety	angle
Compound I			
CU ₁ -N ₄₄ -N ₄₃ -N ₄₂	-63.90(6)	CU ₁ -N ₁₂ -N ₁₃ -N ₁₄	-38.78(6)
CU ₆ - N ₄₂ -N ₄₃ -N ₄₄	-168.21(7)	CU ₂ - N ₁₂ -N ₁₃ -N ₁₄	168.84(6)
CU ₇ - N ₄₂ -N ₄₃ -N ₄₄	-40.67(7)	CU ₃ - N ₁₂ -N ₁₃ -N ₁₄	58.05(6)
		CU ₇ - N ₁₄ -N ₁₃ -N ₁₂	71.20(6)
Compound II			
CU ₁ -N ₄₄ -N ₄₃ -N ₄₂	-79.51(45)	CU ₁ -N ₁₂ -N ₁₃ -N ₁₄	-26.78(43)
CU ₆ - N ₄₂ -N ₄₃ -N ₄₄	-157.90(44)	CU ₂ - N ₁₂ -N ₁₃ -N ₁₄	177.53(41)
CU ₇ - N ₄₂ -N ₄₃ -N ₄₄	-24.95(46)	CU ₃ - N ₁₂ -N ₁₃ -N ₁₄	68.81(42)
		CU ₇ - N ₁₄ -N ₁₃ -N ₁₂	69.65(45)

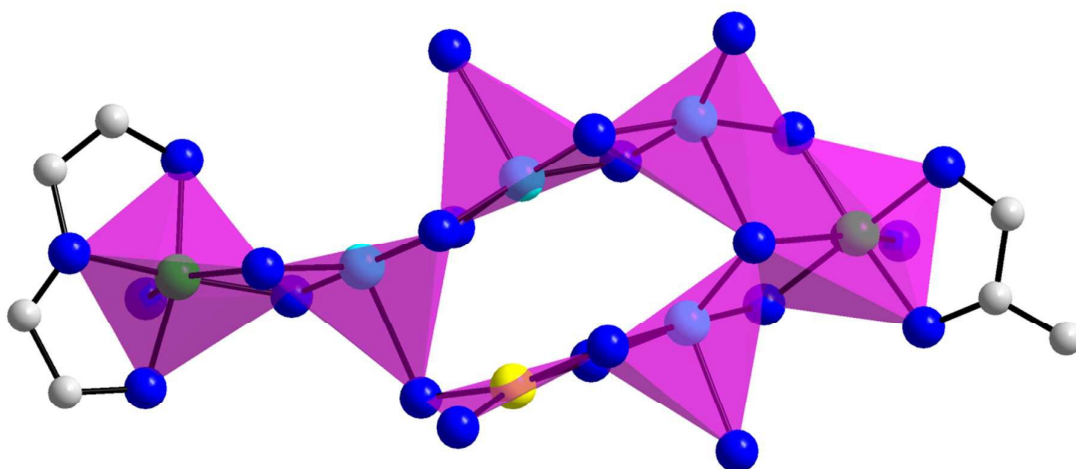


Figure 1: (a) View of heptanuclear Cu^{II} unit. (Octahedral, square pyramidal and square planar metal centers are represented by green, cyan and yellow colours, respectively).

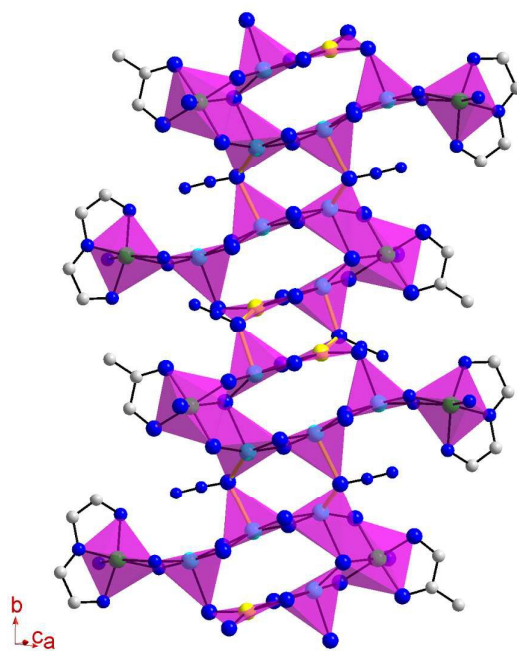


Figure 2: View of ribbon-like 1D chain of Cu_7 unit in compound **I** along the crystallographic axis c .

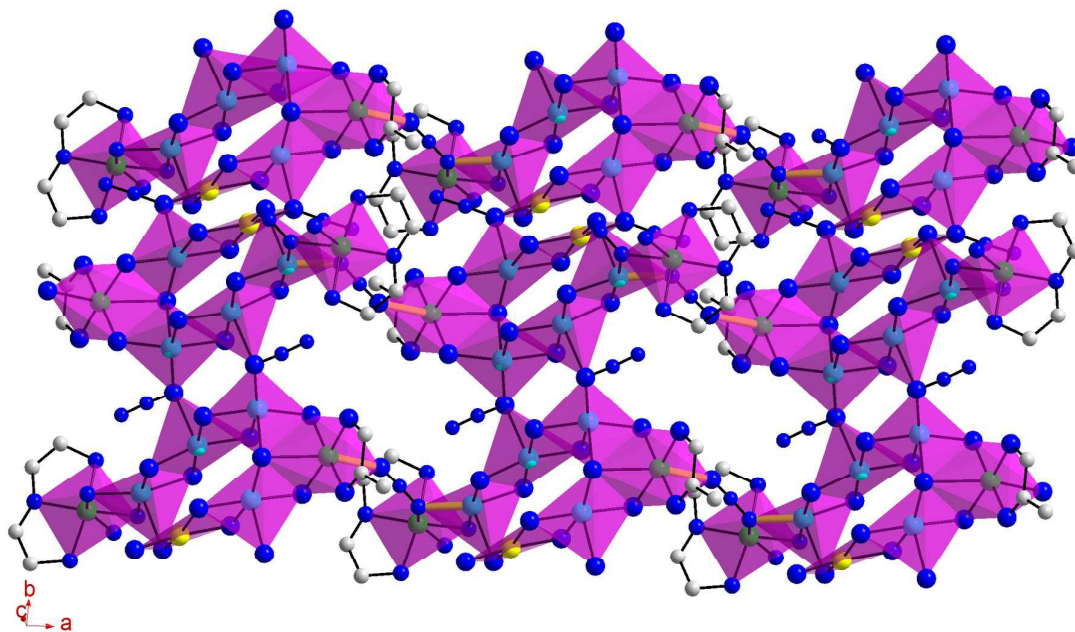


Figure 3: View of 2D layer of Cu_7 unit in compound **I** along the crystallographic axis c .

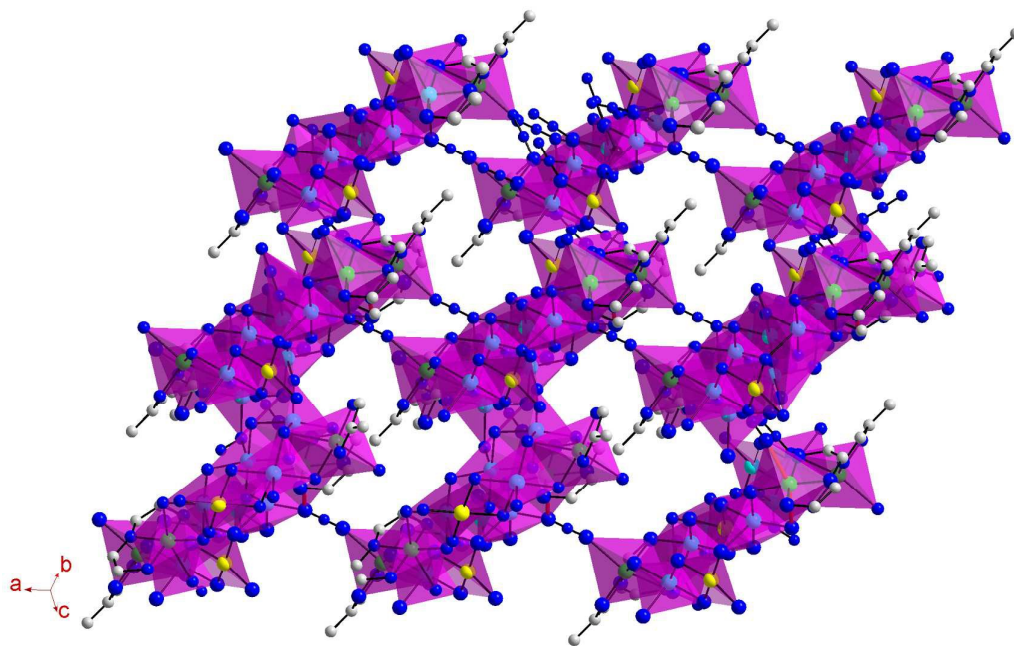
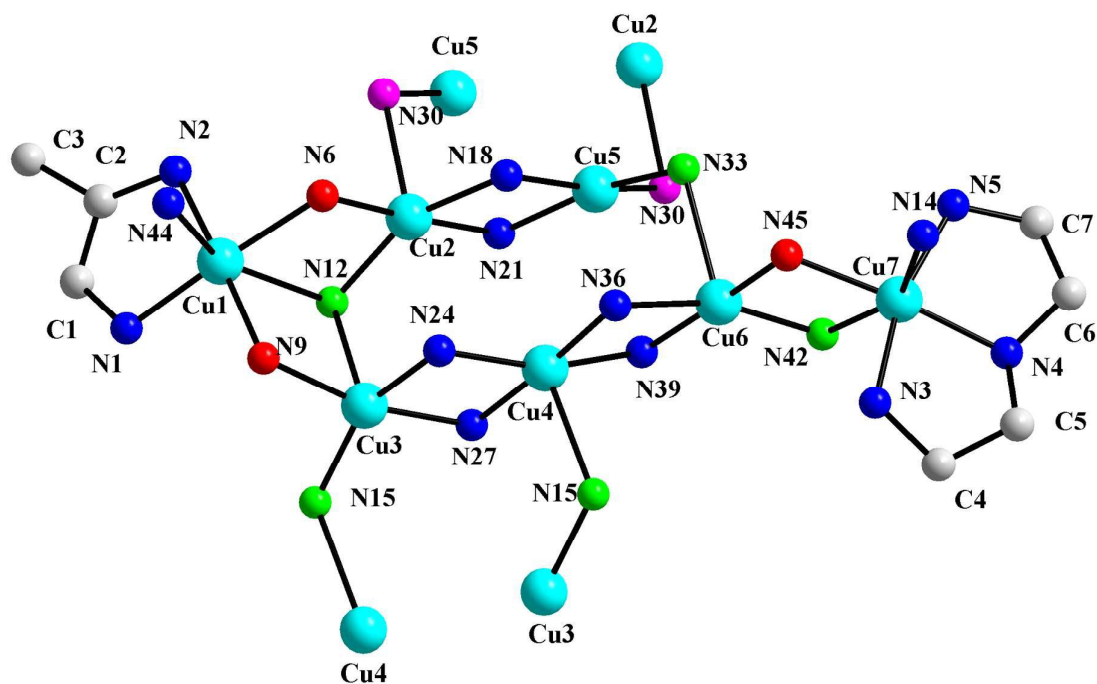
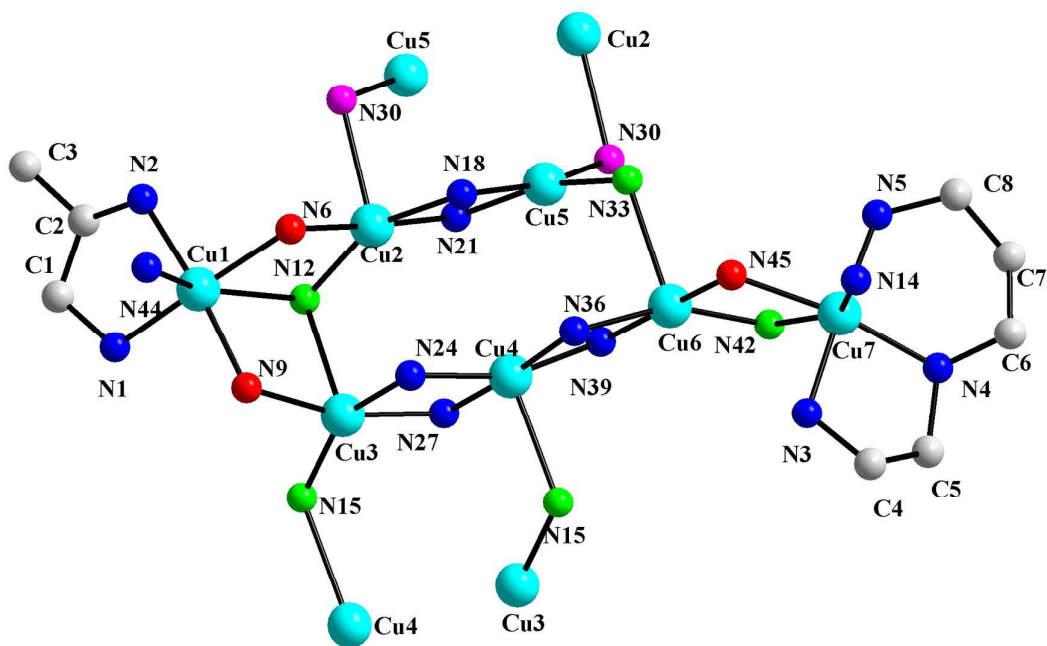


Figure 4: View of the 3D structure of $[\text{Cu}_7(\text{N}_3)_{14}(\text{C}_3\text{H}_{10}\text{N}_2)(\text{C}_4\text{H}_{13}\text{N}_3)]_n$ (I)



(a)



(b)

Figure 5: View of probable magnetic interaction within the Cu₇ unit in compound (a) **I** and (b) **II**. Blue: Ferromagnetic interactions (< 105°); Red: Anti-Ferromagnetic interactions (>105°) Pink: Border line (105°) exchanges; even if it is weak would be a be Ferromagnetic interaction between the Cu₇ units. Green: Very weak or no exchanges either (F or AF). (See text and table S3-S4)

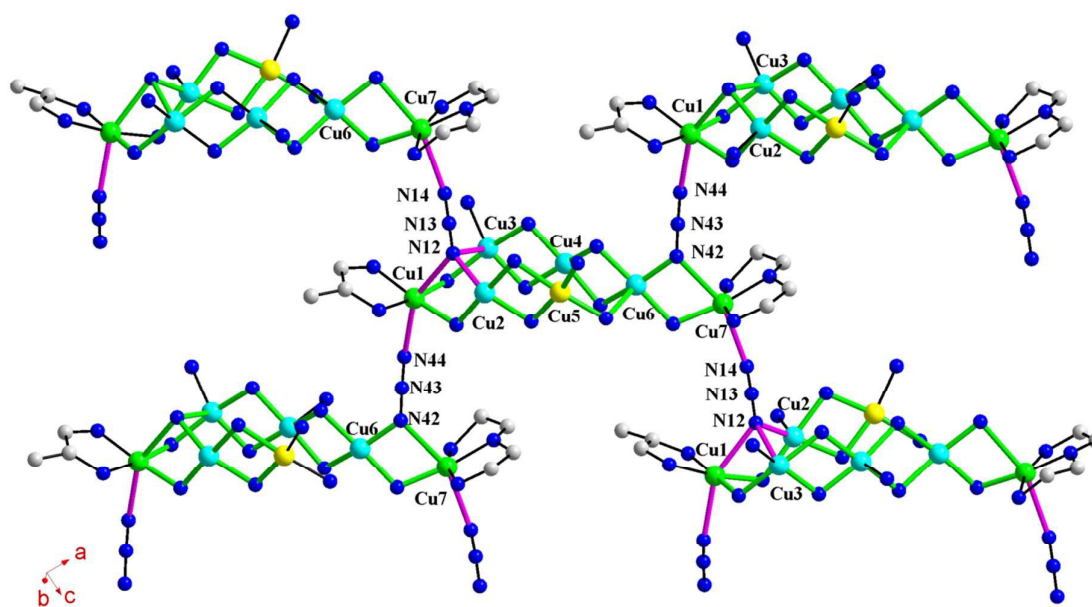


Figure 6: Figure shows the Cu7 connectivity via the (E,O) bridging of the azide (See text).

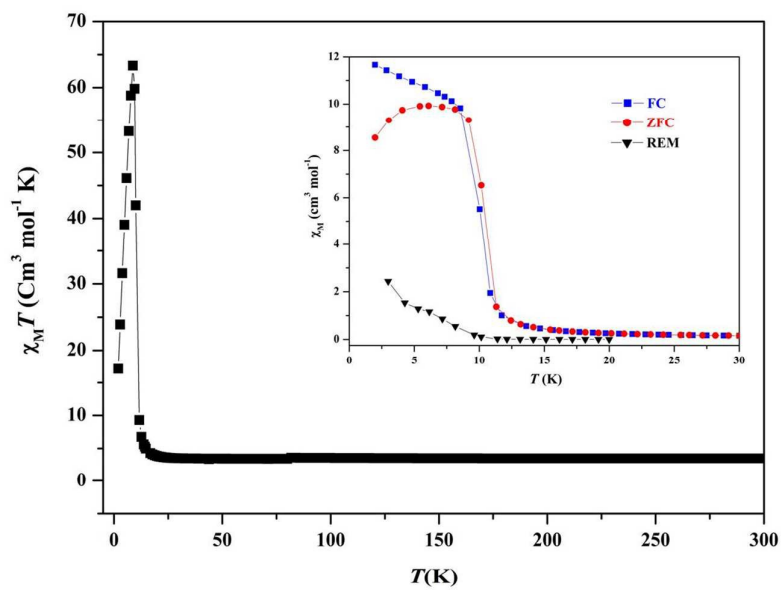


Figure 7: Temperature dependence of $\chi_M T$ for compound **I** (the susceptibility down to 80 K has been collected with a field $H_{\text{DC}} = 1 \text{ kOe}$ while below 80 K data have been obtained for $H_{\text{DC}} = 50 \text{ Oe}$), and (inset) FC, ZFC and REM behavior (reference field $H_{\text{DC}} = 50 \text{ Oe}$).

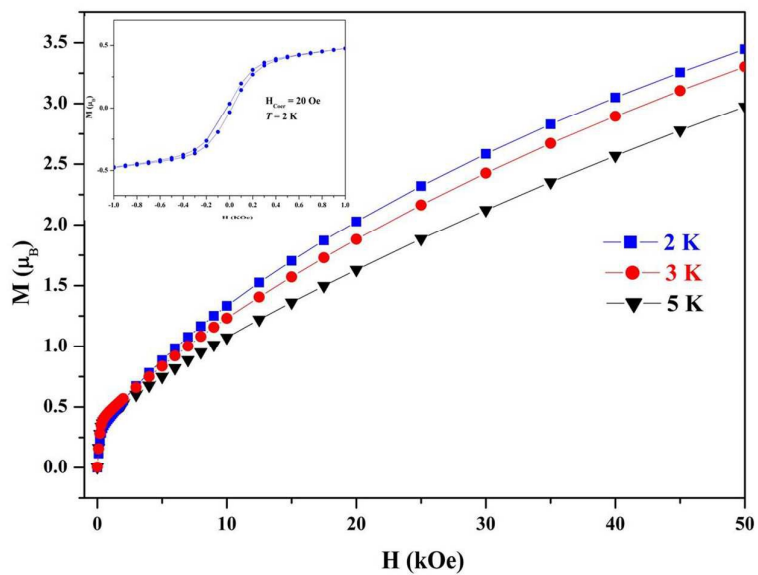


Figure 8: Field dependence of the magnetization for **I** at 2, 3, and 5 K and (inset) hysteresis loop with $H_{coer} = 20$ Oe observed at 2 K.

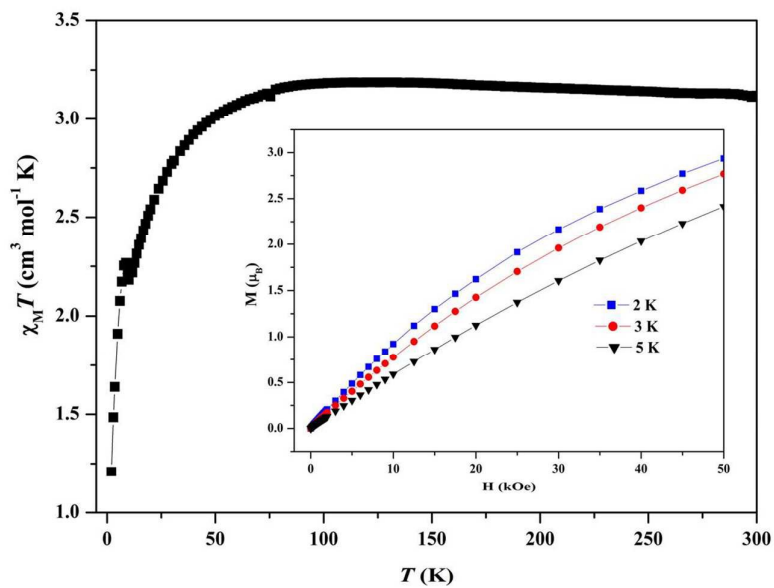


Figure 9: Temperature dependence of $\chi_M T$ for compound **II** and (inset) field dependence of the magnetization at 2, 3, and 5 K.

Stabilization of Cu₇ Clusters in Azide networks: Syntheses, Structures and Magnetic behaviours

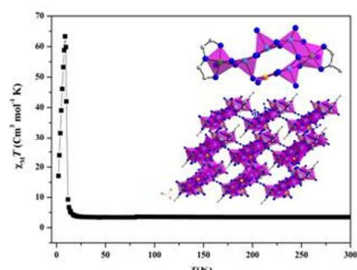
Subhradeep Mistry, Jean-Pascal Sutter^{2,3} and Srinivasan Natarajan¹

¹ Framework solids laboratory, Solid State and Structural Chemistry unit, Indian Institute of Science, Bangalore-560012, India.

² CNRS ; LCC (Laboratoire de Chimie de Coordination) ; 205, route de Narbonne, F-31077 Toulouse, France

³ Université de Toulouse ; UPS, INPT ; LCC ; F-31077 Toulouse, France

Table of Contents



Two Cu^{II} azide compounds having Cu₇ clusters have been prepared, by employing two different blocking amines with different denticity, and their magnetic behaviour described and discussed.

¹ E-mail: snatarajan@sscu.iisc.ernet.in; jean-pascal.sutter@lcc-toulouse.fr